HOLOGIC®
The Science of Sure

Powerful images.
Clear answers.

Manage Patient's concerns about Atypical Femur Fracture*

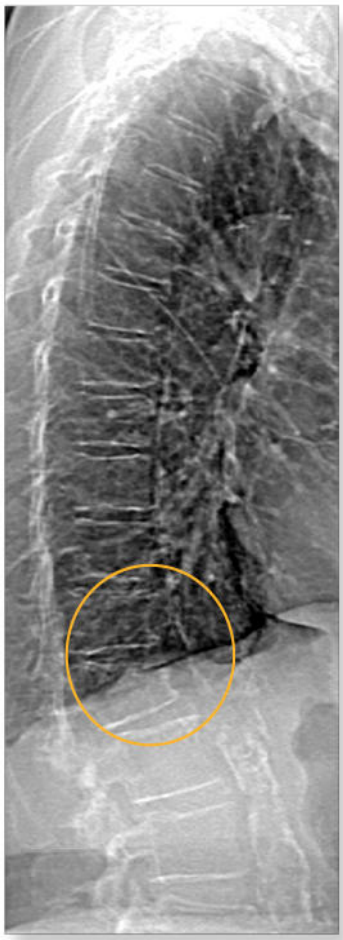

Vertebral Fracture Assessment – a critical part of a complete fracture risk assessment

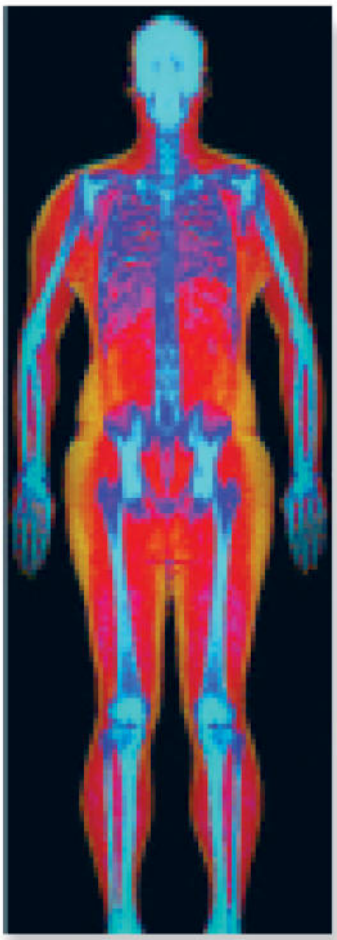

Advanced Body Composition® Assessment – the power to see what's inside

Contact your Hologic rep today at BSHSalesSupportUS@hologic.com

*Incomplete Atypical Femur Fractures imaged with a Hologic densitometer, courtesy of Prof. Cheung, University of Toronto

www.hologic.com | dxaperformance.com | 1.800.442.9892

Type-I Angiotensin II Receptor Blockade Reduces Uremia-induced Deterioration of Bone Material Properties

Takuya Wakamatsu [1†], Yoshiko Iwasaki [2†], Suguru Yamamoto [1], Koji Matsuo [1], Shin Goto [1], Ichiei Narita [1], Junichiro J. Kazama [3], **Kennichi Tanaka [3]**, Akemi Ito [4], Ryosuke Ozasa [5], Takayoshi Nakano [5], Chisato Miyakoshi [6,7,8], Yoshihiro Onishi [7], Shingo Fukuma [6,9], Shunichi Fukuhara [6,8], Hideyuki Yamato [10], Masafumi Fukagawa [10], Tadao Akizawa [11]

[1] Division of Clinical Nephrology and Rheumatology, Niigata University Graduate School of Medical and Dental Sciences, Niigata, Japan

[2] Department of Health Sciences, Oita University of Nursing and Health Sciences, Oita, Japan

[3] Department of Nephrology and Hypertension, Fukushima Medical University, Fukushima, Japan

[4] Ito Bone Histomorphometry Institute, Niigata, Japan

[5] Division of Materials and Manufacturing Science, Graduate School of Engineering, Osaka University, Suita, Japan

[6] Department of Healthcare Epidemiology, School of Public Health in the Graduate School of Medicine, Kyoto University, Kyoto, Japan

[7] Department of Pediatrics, Kobe City Medical Center General Hospital, Kobe, Japan

[8] Institute for Health Outcomes and Process Evaluation Research (iHope International), Kyoto, Japan

[9] The Keihanshin Consortium for Fostering the Next Generation of Global Leaders in Research (K-

This article has been accepted for publication and undergone full peer review but has not been through the copyediting, typesetting, pagination and proofreading process which may lead to differences between this version and the Version of Record. Please cite this article as doi: 10.1002/jbmr.4159

CONNEX), Kyoto, Japan.

[10] Division of Nephrology, Endocrinology and Metabolism, Tokai University School of Medicine, Isehara, Japan

[11] Division of Nephrology, Department of Medicine, Showa University School of Medicine, Tokyo, Japan

[†]: T.W. and Y.I. contributed equally to this work.

Running Title: AT-1RB and Uremic Bone

[*]Corresponding author: Junichiro J. Kazama,

Department of Nephrology and Hypertension, Fukushima Medical University,

1 Hikarigaoka, Fukushima, Fukushima, 960-1295 JAPAN

TEL +81-24-547-1206

Email jjkaz@fmu.co.jp

Disclosure

The MBD-5D study was financially supported by Kyowa Kirin Co., Ltd (KK). S.Y. has received honoraria from KK. S. Fukuma has acted as a scientific advisor for KK. TA has received consulting fees from KK, Astellas Pharma, Bayer, Fuso Pharmaceutical, Japan Tobacco, Ono Pharmaceutical,

Otsuka, Sanwa, GSK and NIPRO; and lecture fees from KK, Chugai Pharmaceutical, Bayer, Kissei Pharmaceutical, Japan Tobacco, and Ono Pharmaceutical. S. Fukuhara has acted as a scientific advisor for and has received grants from KK. MF has received consulting fees from KK and Ono Pharmaceutical; lecture fees from KK, Bayer, Kissei Pharmaceutical, Japan Tobacco, and Ono Pharmaceutical; and grants from KK and Bayer. JJK has received lecture fees from KK, Japan Tobacco, Chugai Pharmaceutical, Kissei Pharmaceutical, and Ono Pharmaceutical. The remaining authors have no conflicts to report.

Abstract

Chronic kidney disease (CKD) is associated with a high incidence of fractures. However, the pathophysiology of this disease is not fully understood, and limited therapeutic interventions are available. This study aimed to determine the impact of type-1 angiotensin II receptor blockade (AT-1RB) on preventing CKD-related fragility fractures and elucidate its pharmacological mechanisms. AI-1RB use was associated with a lower risk of hospitalization due to fractures in 3276 patients undergoing maintenance hemodialysis. In nephrectomized rats, administration of olmesartan suppressed osteocyte apoptosis, skeletal pentosidine accumulation and apatite disorientation, and partially inhibited the progression of the bone elastic mechanical properties, while the bone mass unchanged. Olmesartan suppressed angiotensin II-dependent oxidation stress and apoptosis in

primary cultured osteocytes *in vitro*. In conclusion, angiotensin II-dependent intraskeletal oxidation stress deteriorated the bone elastic mechanical properties by promoting osteocyte apoptosis and pentosidine accumulation. Thus, AT-1RB contributes to the underlying pathogenesis of abnormal bone quality in the setting of CKD, possibly by oxidative stress.

Keywords

Chronic kidney disease, bone material properties, renin-angiotensin-aldosterone system, olmesartan

Introduction

Chronic kidney disease (CKD) induces systemic mineral metabolism abnormalities, which constitute a condition termed CKD-mineral and bone disorder (CKD-MBD). [1] Although many nephrologists believe that parathyroid dysfunction is the main cause of fragility fractures in CKD patients, clinical studies have failed to provide evidence to make a consensus on this issue. [2-5] Some studies even found no significant association between parathyroid function and fracture risk, [6, 7] while there seems to be no argument regarding the elevated risk of fractures in CKD patients. [8-12]

Experimental kidney damage has been shown to induce abnormal bone mechanical properties without reducing the bone mass in animal models.[13-15] The severity of these abnormalities was associated with the level of uremic toxins, [13, 14] but not with the parathyroid hormone (PTH) level. [14]

Osteoblasts express type 1 angiotensin II receptors (AT-1R) [16], which assist osteoclastogenesis by promoting the receptor activator for nuclear factor kB ligand. [17] Therefore, an AT-1R blockade (AT-1RB) may have the potential to suppress osteoclastic bone resorption. A previous observational clinical study showed that the administration of renin-angiotensin-aldosterone system inhibitors (RASi) including AT1-RB, was associated with an approximately 30% lower risk of hospital admission due to any fracture among patients with secondary hyperparathyroidism undergoing

hemodialysis.[18] The effect of RASi on preventing fractures in patients with CKD seemed more evident than that in the general population;[19] however, the reason behind this finding remains unknown.

In this study, we aimed to determine the impact of AT-1RB administration on preventing fragility fractures in patients undergoing hemodialysis and to elucidate the pharmacophysiological mechanisms underlying its preventive effect against bone fragility, with a special focus on the bone material properties.

Materials and Methods

Clinical study

Study design

The MBD-5D study was a multicenter, prospective, observational study designed to follow patients with secondary hyperparathyroidism receiving maintenance hemodialysis for 3 years. Details of the study design have been reported previously.[20] In short, the MBD-5D study followed 8,229 patients from January 2008 to January 2011. Forty percent (n=3,276) of patients were randomly selected as a subcohort, and their data were used in this analysis. The mean observation period was

2.74 years; all study procedures were conducted in accordance with the Declaration of Helsinki. Because this was an observational study of anonymized data collected during routine practice, informed consent from subjects was not mandatory according to the ethical guidelines for epidemiological research in Japan. The study protocol and the informed consent waiver were approved by the central ethics committee at Kobe University (no. 754).

Inclusion and exclusion criteria

Patients undergoing maintenance hemodialysis at a participating facility as of January 1, 2008, and who satisfied any of the inclusion criteria (intact PTH (iPTH) level of ≥180 pg/mL or treatment with intravenous vitamin D receptor activator or oral active vitamin D receptor activator) were eligible to participate. Patients undergoing hemodialysis for <3 months were excluded.

Outcomes and exposure

The outcome of interest in this study was the time to hospitalization due to any type of fracture. The period from the start of observation to the occurrence of the first event was recorded. Hospitalization for a fracture at any site was designated as "any fracture", ; if medical record review indicated a hip fracture, this subset was designated as "hip fracture". A participant was considered to

be censored when time-to-event information was not available due to loss to follow-up or occurring of the initial event. The exposure of interest was the use of AT1-RB at study onset. All data were obtained from each patient's medical record.

Statistical processing

The distributions of continuous and categorical variables are presented as median (interquartile range) and percentages, respectively. The baseline characteristics of patients were compared between those hospitalized due to any fracture and those not hospitalized, employing a t-test or chi-squared test for continuous and categorial variables, respectively.

To investigate the association between factors including the use of AT1-RB and incidence of hospitalization due to any fracture, and that due to hip fracture, multivariable-adjusted Cox proportional hazard models were used to estimate the hazard ratios (HRs) and their 95% confidence intervals (CIs). The following covariates were included in the model: age; sex; body mass index; cause of end-stage kidney disease; diabetes mellitus; history of cardiovascular disease; history of parathyroidectomy; duration of dialysis; urea removal during a hemodialysis session (Kt/V); serum levels of albumin, calcium, phosphorus, intact parathyroid hormone (iPTH), and alkaline phosphatase (ALP); use of AT1-RB; and use of other antihypertensives, vitamin D receptor activators and

phosphate binders. CKD-MBD levels were categorized as follows: calcium, <8.4 g/dL, 8.4-10.0 g/dL, and >10 g/dL; phosphorus, <3.5 g/dL, 3.5-6.0 g/dL, and >6.0 g/dL; iPTH, <60 pg/mL, >60 - <240 pg/mL, >240 - <500 pg/mL, and >500 pg/mL; [21] and ALP, four categories according to quartiles.

All analyses were performed using SAS 9.2 and differences with $P<0.05$ were considered significant.

Experimental studies

Materials

Alfa-minimal essential medium (α-MEM), penicillin 100 units/ml, and streptomycin 100 µg/ml were purchased from Life Technologies (Grand Island, NY). Fetal bovine serum (FBS) and calf serum (CS) were purchased from HyClone Laboratories (Logan, UT). Olmesartan was kindly supplied by Daiichi-Sankyo Pharmaceutical Co. Ltd (Tokyo, Japan). Hydralazine and angiotensin II were purchased from Sigma (St. Louis, MO). The fluorescent probe 2',7'-dihydro-fluorescein diacetate (Molecular Probes, Eugene, OR, USA) was purchased from Invitrogen (Shibaura, Tokyo, Japan).

In vivo study

Animal care

This study was approved by the Institutional Review Board of the Niigata University Hospital, Niigata, Japan (#269-1). Sprague-Dawley male rats were maintained at a room temperature of 21-24 ℃, humidity of 30-35 % and light and dark cycles of 12 h each (8:00 a.m. to 8:00 p.m. in light and 8:00 p.m. to 8:00 a.m. in the dark). Until the age of 13 weeks, the rats were kept on a standard diet (MF; 1.07 % calcium, 0.83 % phosphorus) (Oriental Yeast Co. LTD, Japan); at the age of 14 weeks, the rats were started on a special formula diet (CE-2; 2.0% calcium, 1.0% phosphorus) (CLEA Japan, Tokyo, Japan). Rats were allowed ad libitum access to food and tap water. At the age of 14 to 15 weeks, the rats underwent a sham operation (group C) or a 5/6 subtotal nephrectomy under general anesthesia with isoflurane. More precisely, they underwent a total right nephrectomy and a 2/3 left nephrectomy with a 1-week interval. At the age of 21 weeks, 5/6 nephrectomized rats were distributed into three groups, the NO, NH, and N groups, and were administered olmesartan (RNH-6270) (3 mg/kg/day), hydralazine hydrochloride (10 mg/kg/day), and saline, respectively, using Alzet osmotic mini pump model 2ML2 (Alza). Olmesartan and hydralazine hydrochloride (model 2ML2) pumps were exchanged every 2 weeks. The body weight, blood pressure, and pulse rate of the rats were recorded at 26 weeks of age. Systolic, diastolic and mean blood pressure and pulse rates were measured using the tail-cuff method with heating, as previously described. [22] Briefly, rats were pre-heated in a chamber at 39 °C for 10 min. A cuff with a pneumatic pulse sensor was attached to the tail (BP-98A-

L; Softron Beijing Incorporated, Beijing, China). Blood pressure and pulse rate values were averaged from at least four consecutive readings in each rat. Rats at the age of 27 weeks were deeply anesthetized with isoflurane and sacrificed to collect femurs and blood for biochemical analysis.

Measurement of biochemical parameters:

Blood was centrifuged for 20 minutes at 3000 rpm and serum samples were used to determine urea nitrogen, creatinine, calcium and inorganic phosphorus levels (SRL, Inc. Tokyo, Japan). Plasma was separated using EDTA-2Na and centrifuge for 15 minutes at 1600×g; the supernatant was used for measurement of plasma intact PTH concentration using an ELISA Kit (Immutopics, San Clemente, CA) according to the manufacturer's instructions.

Bone mineral densitometry (BMD)

The BMD values of the right femur were measured by dual-energy X-ray absorptiometry (Aloka DCS-600R; Aloka Co., Tokyo, Japan).

Bone Histomorphometry

The left femur of each rat was collected and fixed in 70% ethanol. The fixed femurs were

stained with Villanueva Bone Stain Solution for 6 days en bloc, and thereafter embedded into a methyl methacrylate resin. The histomorphometry of cancellous bone fields at 320× magnification in each specimen was analyzed. The results were expressed according to previously described methods. [24, 25]

Dynamic mechanical analysis (DMA)

DMA was performed as described previously. [13-15] Briefly, each right femur that was used for BMD measurement was placed in a DMA device (DMA 7e; PerkinElmer, Norwalk, CT), and the baseline viscoelasticity was measured in a 0.9% saline solution at 37 °C by an oscillatory test using a 3-point bending configuration. Before DMA, the thickness and width were measured at the center of each femur. The femur sample was then placed in the DMA device to determine the standard DMA profile. Scanning frequencies ranged from 0.1 to 25 Hz (in 0.2 Hz increments). The test was conducted under displacement control. The storage modulus E1, (obtained from dynamic testing, equivalent to Young's modulus) was measured for each sample. [15]

Confocal Raman spectroscopic measurements

Each femur sample used for DMA measurement was cut at the center of the diaphysis. Each cross-sectional surface was polished and smoothed. A Nicolet Almega XR Dispersive Raman

microscope system equipped with the OMNIC Atlus TM imaging software (Thermo Fisher Scientific, Auburn, AL) was used to examine the composition and relative amounts of minerals and bone matrix, as previously described. [13-15] Three cross-sectional surfaces (anterior, posterior and interior of the femur, as previously described [16] were irradiated using a high-brightness, low-intensity laser operating at 780 nm. Raman spectral images were acquired and the average values of the three points were calculated. Each parameter was calculated as follows; the relative bone mineral amount was estimated by the v1 phosphate stretching vibration at 950-964 cm^{-1}. In the same way, the relative bone matrix amount was estimated by amide Ⅲ（1242 -1269 cm^{-1}). The carbonate/phosphate ratio was calculated as the ratio of the band area of type B carbonate substitution (1065-1070 cm^{-1}) to v1 phosphate substitution (950-964 cm^{-1}). Collagen maturity was calculated as the ratio of 1660 cm^{-1} (mature collagen) to 1690 cm^{-1} (immature collagen). The amount of pentosidine was estimated as the sum of the band areas that peaked at 1305 cm^{-1} and 1362 cm^{-1}. For each sample, three averaged Raman spectral images were acquired in the middle of the anterior cortical bone from the femoral cross-sectional surface (each image was acquired using 10 times measurements) and the mean values were calculated.

In vitro Study

Osteocytes preparation

Primary osteocytes were isolated from mouse hindlimb bones, according to the combined methods of Mikuni-Takagaki et al. [(25))] and Stern et al. [(26)] with some modifications. Briefly, the hindlimb long bones (femur and tibia) were aseptically dissected from 10-week-old Institute of Cancer Research mice (SRL, Hamamatsu, Japan). The bones were minced into 1mm pieces and serial digested with 1mg/ml collagenase (Wako, Osaka, Japan) 5 times for 20 min each in α-MEM at 37℃. The cells were then collected through a 100-μm nylon cell strainer. Cells of the first and second fractions were discarded as these fractions contains abundant fibroblastic cells. Cells from fractions 3 to 5 were pooled as osteoblast-rich fractions. Residual bone pieces were treated with 4mM EGTA in Ca^{2+}-free, Mg^{2+} -free Hanks' balanced salt solution for 15minutes (fraction 6) and 1 mg/ml collagenase for 20minutes (fraction 7) to collect the cells. These digestions were repeated until fraction 11 was obtained. Fractions 6 and 7 (fraction 6/7), 8 and 9 (fraction 8/9) and 10 and 11 (fraction 10/11) were combined because of the low cell number. We performed a real-time polymerase chain reaction (PCR) analysis using RNA extracted from 4 day-cultured cells in fractions 3 to 10/11 to examine the expressions of osteoblast and osteocyte marker genes (Supplemental Figure1). Keratocan was the marker gene of osteoblasts, [(29)] while SOST and FGF23 were the marker genes of osteocytes. Keratocan was strongly expressed in fraction 3, whereas the opposite was seen in fraction 8/9 and 10/11. However, the expression of SOST

was higher in fraction 6/7 8/9, and 10/11. FGF23 gene expression was higher in fraction 8/9 and 10/11 than in fraction 3, which also had the lowest SOST expression. These results were in agreement with those of a previous study, [21] and we confirmed fraction 3-5 as osteoblast-rich and fraction 6/7, 8/9, and 10/11 as osteocyte-rich. Osteocytic cells were cultured on type-I collagen-coated plates (Becton Dicknson, Franklin Lakes, NJ) at a seeding density of 2×10^6 cells/9cm^2 in α-MEM supplemented with 5% FBS and 5% CS, penicillin 100 units/ml, and streptomycin 100 μg/ml.

RNA isolation, cDNA synthesis and PCR analysis

To confirm the successful isolation of osteoblasts and osteocytes from mouse hindlimb long bones, we analyzed the gene expression in cultured cells. Five days post-isolation, the total RNA was isolated from plated cells using the RNeasy Mini Kit (QIAGEN, Tokyo, Japan) according to the manufacturer's instructions. The total RNA (1 μg) was used as the template for cDNA synthesis with a 20-μl volume using an RT-PCR kit (Invitrogen) according to the manufacturer's instructions. Real-time PCR was performed using 1μL of cDNA with a 20-reaction volume using StepOne plus (Applied Biosystems, Waltham MA). We used SYBR Green chemistry to determine the mRNA levels of SOST, FGF23, keratocan, and a housekeeping gene, beta-actin. The double-stranded DNA-specific dye SYBR Green I was incorporated into the PCR buffer provided in the SYBR Green Real-time PCR

master Mix (Toyobo Co. Ltd., Tokyo, Japan) to enable quantitative detection of products. The PCR conditions were 95℃ for 30seconds, 40 denaturation cycles at 94℃ for 5 seconds, and annealing and extension at 60℃ for 30 seconds.The primer sequences used are shown in supplemental Table 1. Beta-actin was used to normalize the differences in reverse transcription efficiency. We also assessed *AT-1R* gene expression and determined the effect of AT-1RB on angiotensin II-induced NADPH oxidase gene expression.

Assessment of reactive oxygen species (ROS) production

Intracellular ROS were quantified as previously described. [27, 28] Primary osteocytic cells were seeded into a 96-well microplate at a density of 2×10^4 cells/well. After incubation for 4 days, the osteocytes were washed with D-PBS. Then 100 μl of D-PBS containing 5 mM D-glucose and 20 μM DCFH-DA together with various concentrations (0 to 1000nM) of angiotensin II were added to the wells. Olmesartan (10 mM), hydralazine (30mM) or vehicle was simultaneously added to the wells. Immediately after the addition and after incubation at 37°C for 120 min, the fluorescence intensity was analyzed using a fluorescence plate reader (Spectromax Gemini XS, Molecular Devices, Sunnyvale, CA) at excitation/emission wavelengths of 485/535 nm. Data were expressed as percent increase in fluorescence intensity compared to the untreated control. ROS production was also

determined in the presence of 10μM olmesartan, 30μM hydralazine, 2.5mM N-acetyl cysteine, or 0.5 μM diphenyleneiodonium.

Measurement of cell viability

Cell viability was evaluated using an MTT (3-[4,5-dimethylthiazol-2-yl]-2,5-diphenyl-tetrazolium bromide) assay (Dojin Chemicals, Kumamoto, Japan) as described previously.[29] Primary osteocytic cells (2×10^4 cells/well) were inoculated into 96-well microplates. After culturing for 4days, various concentrations (0 to 1000 nM) of angiotensin II were added and the cells were incubated at 37°C for 24 to 96 h. Then the cells were lysed with isopropanol/HCl solution, and the absorbance of each well was measured at 570 nm with absorbance at 630 nm as reference, using a microplate reader (SpectraFluor; Tecan, Austria). We also examined the effect of olmesartan, hydralazine, and antioxidants on cell viability with 1000 nM of angiotensin II.

Measurement of DNA fragmentation

For the assessment of apoptosis-induced DNA fragmentation, osteocytic cells were seeded in a 96-well microplate at a density of 2×10^4 cells/well and incubated at 37°C for 4days. Various concentrations (0 to 1000 nM) of angiotensin II were added and the cells were incubated for a further

48 h. DNA fragmentation was assessed using the Cellular DNA Fragmentation ELISA Kit (Roche Diagnostics, Basel Switzerland) according to the manufacturer's instructions.

Statistics

All data were expressed as mean ± standard deviation. The data was statistically analyzed by the Mann-Whitney U test. Analyses were performed using SAS 9.2 and differences with $P<0.05$ were considered significant

Results

The association between AT-1RB use and fractures in patients undergoing hemodialysis

During the observation period, 178 (5.4%) of the 3,276 patients were hospitalized due to fracture, of which 58 were due to a hip fracture. The baseline characteristics of the participants are shown in Table 1. All baseline covariates included in the regression model were retrospectively collected from medical records, and there were no missing data.

The median age of patients was 63 (54-71) years. More than 60% were male. The mean age of

patients hospitalized due to fracture was higher than that of those who were not (68.1 years vs. 61.6 years, *P<0.001*). Among those hospitalized for fracture, the proportion of female patients was 50.6%, which was higher than that in patients not hospitalized (37.8%, *P=0.001*). Additionally, the body mass index was lower in patients with fractures than in those without fractures.

AT-1RB use was lower in patients hospitalized due to fractures than in those without fractures (24.7% vs 36.0%, *P=0.002*). The results of Cox regression analyses with respect to the patients' background data are shown in Figure 1. AT-1RB use also showed an association with a lower risk of hospitalization due to any fracture (HR 0.57, 95% CI 0.40-0.81, *p<0.01*) (Figure 1A) and hip fractures (HR 0.37, 95% CI. 0.19-0.73, *p<0.01*) (Figure 1B), while the use of vitamin D receptor activators (VDRA) and phosphate binders did not show any association with hospitalization due to fractures.

Effect of olmesartan use on kidney damage-induced deterioration of bone material properties in vivo

Forty-six animals (group C: 6, N: 14, NO: 13, NH:13) were included in the experiment, and 17 (group C: 0, N: 6, NO: 4. NH:7) died during the observation period because of uremia. The remaining 29 were subjected to the analyses. Results of the *in vivo* study are summarized in Table 2. Nephrectomized rats showed a significant loss of body weight, which was not improved by treatment with olmesartan or hydralazine. Significant hypertension was found in rats in group N; treatment with

either olmesartan or hydralazine decreased the blood pressure to similar values to those in group C. In the biochemical analyses, azotemia and hyperparathyroidism was significantly increased in the nephrectomized groups and treatment with anti-hypertensive drugs showed no effect. Femoral bone density significantly decreased in nephrectomized rats, and treatment with anti-hypertensive drugs did not improve osteopenia.(Table 2) Bone histomorphometric testing revealed an increased tendency in eroded surfaces and osteoclastic numbers that enhanced bone resorption and osteoblastic/osteoid surfaces that enhanced bone formation in nephrectomized groups. There was no difference in these parameters among the three nephrectomized groups.

DMA of femurs showed that nephrectomized rats had significantly decreased storage module levels than those in group C (N: $2.5x10^9 \pm 7.9x10^8$ pa vs C: $7.7x10^9 \pm 2.5x10^8$ pa, $P<0.05$). Treatment with olmesartan, but not with hydralazine, partly limited the deterioration (NO: $3.5x10^9 \pm 4.6x10^8$ pa vs NH: $1.5x10^9 \pm 8.3x10^8$ pa, $P<0.05$). (Table 2) Nephrectomy caused an increase in the number of empty lacunae in the cortical bone (N: $55.3 \pm 22.3/mm^2$ vs C: $18.3 \pm 4.6/mm^2$, $P=0.021$), while olmesartan use led to a decrease in the number of empty lacunae compared with hydralazine (NO: $36.6 \pm 12.2/mm^2$ vs NH: $67.9 \pm 13.6/mm^2$, $P=0.013$) (Figure 2). X-ray diffraction study revealed significant bone apatite disorientation in nephrectomized rats (N: 5.4 ± 0.6 vs C: 6.9 ± 0.3, $P<0.001$), while treatment with olmesartan treatment improved this value to a level comparable to that in control rats

(NO: 6.8 ± 0.2 vs C: 6.9 ± 0.3, NS).

Results of Raman-spectroscopic analyses are shown in Figure 3. Crystallinity was significantly decreased in nephrectomized rats, which was partially improved by olmesartan treatment (NO: 0.051 ± 0.001 vs N: 0.044 ± 0.001, *P=0.001*). Pentosidine was significantly accumulated in nephrectomized rats, but this effect was countered by treatment with olmesartan. (NO: 0.49 ± 0.08 vs N: 0.81 ± 0.14, *P=0.001*).

Effect of olmesartan use on angiotensin II-induced abnormal osteocyte functions in vitro

When primary cultured osteocytes reacted with angiotensin II *in vitro*, the angiotensin II increased *AT-1R* mRNA expression, (Figure 4) decreased cell viability after 96 h (73.3±2.8% of control, *P<0.001*) (Figure 5) and increased the ROS production (148.2±19.4% of control, *P=0.004*). (Figure 6) Olmesartan, but not hydralazine, ameliorated the angiotensin II-induced impairment of cell viability and ROS production (cell viability: 93.4±8.3% of control, *P=0.011*, ROS production: 114.5±17.4% of control, *P=0.003*). (Figure 7A, B) Angiotensin II increased DNA fragmentation, NADPH oxidase, p22phox and p67phox mRNA expressions in osteocytes, while the opposite effect was seen after olmesartan treatment. (Figure 7C, D and E）

Discussion

Previous clinical studies have suggested that the relationship between fracture risk and PTH levels in patients with CKD patients is unclear. [2-7] Our study also showed that three CKD-MBD markers, including serum levels of PTH, calcium, and phosphorus, were not associated with fracture incidence in patients undergoing hemodialysis (Table 1 and Figure 1). Although recent advancements in treatment with activated vitamin D, calcium-sensing receptor agonists and phosphate binders have contributed to maintaining the circulation levels of the above three CKD markers, [21] the risk of fracture in these patients remains much higher than that in the general population.[8-12]

We focused on the effect of AT-1RB use on hospitalization due to fractures and bone quality in clinical and basic experiments. This clinical observational study revealed that the administration of AT-1RB but not calcium channel blockers was associated with a lower fracture incidence among patients undergoing hemodialysis (Figure 1). Compared with that in a previous study, [19] the effect of AT-1RB seemed to be stronger in patients undergoing hemodialysis than in the general population. In an animal model of experimentally induced kidney injury, intraskeletal protein expression of angiotensin II was significantly increased. [30] If this phenomenon is reproducible in patients with CKD, it may account for the osteoprotective effect of AT-1RB use noted in our study. Hypovitaminosis D is a possible cause of high AII levels in chronic kidney injury *via* the activation of renin gene expression

and subsequent activation of the renin-angiotensin-aldosterone system. [31] Elevated AII levels downregulate renal klotho expression through an AT-1R-dependent manner. [32]

Recent observational studies showed that incidence of hip fractures in patients undergoing hemodialysis is decreasing, [33, 34] which may be due to the increasing use of AT-1RB. However, the pharmacological mechanisms of fragility fracture prevention through AT-1RB use are not known to date. We examined the effect of AT-1RB use on kidney damage-induced bone abnormalities separately from their suppressive effect on osteoclastogenesis.

In animals with experimentally induced kidney injury, although the femoral bone elastic mechanical properties and chemical compositions were shown to be impaired, the administration of olmesartan partially restored these parameters independently of changes in the blood pressure (Table 2 and Figure 2). In contrast, olmesartan did not improve the decrease in bone mass noted in these animals, indicating that the improvement in bone elastic mechanical properties through AT-1RB use is not associated with changes in the bone mass. Although a previous study suggested that the administration of olmesartan was associated with mild suppression of osteoclastic bone resorption, [17] no significant suppressive effect of olmesartan on bone resorption was demonstrated in our study. We do not fully exclude the possibility that olmesartan suppresses bone resorption from this result, but it was at least not sufficient to reduce bone mass in this experimental setting. In contrast, olmesartan restored the uremia-induced

increase in the pentosidine/amide ratio and apatite disorientation, which could contribute to the partial storage modulus increase without the increase in the bone mass. Similar to that noted in previous studies, [13-15] the inhibition of these 2 pathological reactions was due to the direct interaction between the bone and olmesartan. The increased number of empty lacunae observed after kidney damage was also improved on olmesartan administration (Figure 2). An increased number of empty lacunae suggests the promotion of osteocyte death. Thus, the inhibition of the AT-1R with olmesartan partially improved the deterioration of bone elastic mechanical properties without changes in the bone mass in CKD animals.

In the *in vitro* study, the exposure to angiotensin II induced DNA fragmentation, which led to increased osteocyte apoptosis (Figure 7C). Olmesartan inhibited angiotensin II-induced osteocytic functional abnormalities (Figure 7). Angiotensin II is one of the strongest local oxidation stress factors. [35] Thus, the intraskeletal oxidation stress induced by angiotensin II is one of the likely causes of osteocyte death noted in rats with kidney injury. Although the mechanism underlying establishment of apatite orientation is not known to date, it is known that the orientation relies on *in vivo* stress distribution in weight-bearing bones, while the orientation determinants in non-weight-bearing bones have not identified to date. [36] The skeletal load sensor is the osteocyte network. Therefore, a blockade of the osteocyte network by osteocyte apoptosis would dissolve the association between the direction

of *in vivo* stress and apatite orientation, by which bones accommodate the stress imposed upon them. We consider that this is the pathophysiological mechanism by which apatite orientation in weight-bearing bones is affected in patients with CKD. We detected a protective effect of olmesartan on this orientation through the inhibition of osteocyte apoptosis. Previous studies have reported that apatite orientation is affected by the increased osteocyte death observed in osteoporosis due to calcium depletion or abnormalities in the osteocyte network arrangement noted in melanoma bone metastasis, which supports the present assumption. [37] The intraskeletal oxidation stress caused by local angiotensin II production may have also contributed towards the accumulation of advanced glycation end products as a non-physiological type-I collagen crosslink in chronic kidney injury, which is another causative factor for the deterioration in bone material properties. [38]

In summary, we demonstrate that AT-1RB contributes to the underlying pathogenesis of abnormal bone quality in the setting of CKD, possibly by reducing oxidative stress. However, AT-1RB use did not lead to a complete recovery of deteriorated bone elastic mechanical properties or of the level of osteocyte apoptosis. We previously demonstrated that uremic toxins that could be absorbed by oral charcoal absorbents restored bone elastic properties. [14] Angiotensin II would, therefore, be one of those uremic toxins that deteriorate bone elastic mechanical property through promoting local oxidation stress (Figure 6). Recently, it was reported that reduction of total bone AGE using the AGE

crosslink breaker failed to improve bone mechanical properties in animals with chronic kidney injury.[39] We assume they failed because AGE accumulation is not the only pathophysiological mechanism underlying deteriorated bone elastic mechanical properties associated with chronic kidney injury, as this study demonstrated.

There are several limitations of this study. First, a lack of data on bone mass is a limitation of this clinical study. In the animal study, we provided a high-calcium diet to limit the possible effect of PTH on the study results, while significant secondary hyperparathyroidism was still detected in the nephrectomized groups. A previous study reported that parathyroid function was not a factor affecting bone elastic material properties;[14] our study also showed that olmesartan did not affect PTH levels in nephrectomized rats. Even considering the aforementioned limitations, we believe that the study findings are significant.

We found that bone fragility in uremic conditions is not completely caused by a systemic disorder of mineral metabolism. CKD-MBD may not always be the cause of CKD-related bone fragility. Osteoporosis is a skeletal disorder characterized by compromised bone strength predisposing the patients to an increased risk of fracture, [40] regardless of its cause. Reduced bone mass is not a requirement. Therefore, we should consider the cause of fragility fracture in patients with CKD to be osteoporosis, which is possibly caused by multiple factors, such as primary osteopenia, CKD-MBD,

and intraskeletal oxidation stress. [41-43] This study revealed that the administration of AT-1RB is a promising treatment option against intraskeletal oxidation stress and that it partially improves the abnormalities in bone elastic mechanical properties in CKD. Moreover, increased angiotensin II production and intraskeletal oxidation stress was also found in an aged animal model. [44] Administration of AT-1RB, may be a useful treatment strategy for elderly patients with osteoporosis, and further studies are, therefore, warranted on the topic.

References

1. Moe SM, Drueke T, Lameire N, and Eknoyan G. Chronic kidney disease-mineral-bone disorder: a new paradigm. *Adv Chronic Kidney Dis.* 2007;14:3-12.
2. Coco M, Rush H. Increased incidence of hip fractures in dialysis patients with low serum parathyroid hormone. *Am J Kidney Dis.* 2000; 36: 1115-1121.
3. Jadoul M, Albert JM, Akiba T, Akizawa T, Arab L, Bragg-Gresham JL, Mason N, Prutz KG, Young EW, Pisoni RL. Incidence and risk factors for hip or other bone fractures among hemodialysis patients in the Dialysis Outcomes and Practice Patterns Study. *Kidney Int.* 2006; 70: 1358-1366.
4. Ambrus C, Almasi C, Berta K, Deak G, Marton A, Molnar MZ, Nemeth Z, Horvath C, Lakatos P, Szathmari M, Mucsi I. Vitamin D insufficiency and bone fractures in patients on maintenance hemodialysis. *Int Urol Nephrol.* 2011; 43: 475-482.
5. Atsumi K, Kushida K, Yamazaki K, Shimizu S, Ohmura A, InoueT. Risk factors for vertebral fractures in renal osteodystrophy. *American Journal of Kidney Diseases.* 1999; 33: 287–293.

6. Stehman-Breen CO, Sherrard DJ, Alem AM, Gillen DL, Heckbert SR, Wong CS, Ball A, Weiss NS. Risk factors for hip fracture among patients with end-stage renal disease. *Kidney Int.* 2000; 58: 2200-2205.
7. Danese MD, Kim J, Doan QV, Dylan M, Griffiths R, and Chertow GM. PTH and the risks for hip, vertebral, and pelvic fractures among patients on dialysis. *Am J Kidney Dis*. 2006; 47: 149-156.
8. Alem A, Sherrard D, Gillen D, Weiss N, Beresford S, Heckbert S, Wong C, Stehman-Breen C. Increased risk of hip fracture among patients with end-stage renal disease. *Kidney Int.* 2000; 58: 396–399.
9. Wakasugi M, Kazama JJ, Taniguchi M, Wada A, Iseki K, Tsubakihara Y, Narita I. Increased risk of hip fracture among Japanese hemodialysis patients. *J Bone Miner Metab*. 2013; 31: 315-321.
10. Tentori F, McCullough K, Kilpatrick RD, Bradbury BD, Robinson BM, Kerr PG, Pisoni RL. High rates of death and hospitalization follow bone fracture among hemodialysis patients. *Kidney Int.* 2014; 85: 166-173.
11. Maravic M, Ostertag A, Urena P, Cohen-Solal M. Dementia is a major risk factor for hip fractures in patients with chronic kidney disease. *Osteoporosis Int.* 2016; 27: 1665–1669.
12. Hansen D, Olesen JB, Gislason GH, Abrahamsen B, Hommel K. Risk of fracture in adults on renal replacement therapy: a Danish national cohort study. *Nephrology Dialysis Transp.* 2016; 31: 1654–1662.
13. Iwasaki Y, Kazama JJ, Yamato H, Shimoda H, and Fukagawa M. Accumulated uremic toxins attenuate bone mechanical properties in rats with chronic kidney disease. *Bone.* 2013; 57: 477-483.
14. Iwasaki Y, Kazama JJ, Yamato H, Matsugaki A, Nakano T, and Fukagawa M. Altered material properties are responsible for bone fragility in rats with chronic kidney injury. *Bone*. 2015; 81: 247-254.
15. Iwasaki Y, Kazama JJ, Yamato H, and Fukagawa M. Changes in chemical composition of cortical bone associated with bone fragility in rat model with chronic kidney disease. *Bone*. 2011; 48: 1260-1267.
16. Bandow K, Nishikawa Y, Ohnishi T, Kakimoto K, Soejima K, Iwabuchi S, Kuroe K, Matsuguchi T. Low-intensity pulsed ultrasound (LIPUS) induces RANKL, MCP-1, and MIP-1beta expression in osteoblasts through the angiotensin II type 1 receptor. *J Cell Physiol.* 2007; 211: 392-398.

17. Shimizu H, Nakagami H, Osako MK, Hanayama R, Kunugiza Y, Kizawa T, Tomita T, Yoshikawa H, Ogihara T, and Morishita R. Angiotensin II accelerates osteoporosis by activating osteoclasts. *FASEB J.* 2008; 22: 2465-2475.

18. Yamamoto S, Kido R, Onishi Y, Fukuma S, Akizawa T, Fukagawa M, Kazama JJ, Narita I, Fukuhara S. Use of renin-angiotensin system inhibitors is associated with reduction of fracture risk in hemodialysis patients. *PLoS One.* 2015; 10: e0122691.

19. Rejnmark L, Vestergaard P, and Mosekilde L. Treatment with beta-blockers, ACE inhibitors, and calcium-channel blockers is associated with a reduced fracture risk: a nationwide case-control study. *J Hypertens.* 2006; 24: 581-589.

20. Fukuhara S, Akizawa T, Fukagawa M, Onishi Y, Yamaguchi T, Hasegawa T, and Kurokawa K. Mineral and bone disorders outcomes study for Japanese chronic kidney disease stage 5D patients: rationale and study design. *Ther Apher Dial.* 2011; 15: 169-175.

21. Fukagawa M, Yokoyama K, Koiwa F, Taniguchi M, Shoji T, Kazama JJ, Komaba H, Ando R, Kakuta T, Fujii H, , Nakayama M, Shibagaki Y, Fukumoto S, Fujii N, Hattori M, Ashida A, Iseki K, Shigematsu T, Tsukamoto Y, Tsubakihara Y, Tomo T, Hirakata H, Akizawa T; CKD-MBD Guideline Working Group; Japanese Society for Dialysis Therapy. Clinical practice guideline for the management of chronic kidney disease-mineral and bone disorder. *Ther Apher Dial.* 2013; 17: 247-288.

22. Kubota Y, Umegaki K, Kagota S, Tanaka N, Nakamura K, Kunitomo M, and Shinozuka K. Evaluation of blood pressure measured by tail-cuff methods (without heating) in spontaneously hypertensive rats. *Biological & pharmaceutical bulletin.* 2006; 29: 1756-1758.

23. Parfitt AM, Drezner MK, Glorieux FH, Kanis JA, Malluche H, Meunier PJ, Ott SM, Recker RR. Bone histomorphometry: standardization of nomenclature, symbols, and units. Report of the ASBMR Histomorphometry Nomenclature Committee. *J Bone Miner Res.* 1987; 2: 595-610.

24. Dempster DW, Compston JE, Drezner MK, Glorieux FH, Kanis JA, Malluche H, Meunier PJ, Ott SM, Recker RR, Parfitt AM. Standardized nomenclature, symbols, and units for bone histomorphometry: a 2012 update of the report

of the ASBMR Histomorphometry Nomenclature Committee. *J Bone Miner Res.* 2013; 28: 2-17.

25. Mikuni-Takagaki Y, Kakai Y, Satoyoshi M, Kawano E, Suzuki Y, Kawase T, Saito S. Matrix mineralization and the differentiation of osteocyte-like cells in culture. *J Bone Miner Res.* 1995; 10: 231-242.
26. Stern AR, Stern MM, Van Dyke ME, Jahn K, Prideaux M, Bonewald LF. Isolation and culture of primary osteocytes from the long bones of skeletally mature and aged mice. *Biotechniques.* 2012; 52: 361-373.
27. Motojima M, Hosokawa A, Yamato H, Muraki T, Yoshioka T. Uremic toxins of organic anions up-regulate PAI-1 expression by induction of NF-kappaB and free radical in proximal tubular cells. *Kidney Int.* 2003; 63: 1671-1680.
28. Motojima M, Hosokawa A, Yamato H, Muraki T, Yoshioka T. Uraemic toxins induce proximal tubular injury via organic anion transporter 1-mediated uptake. *Br J Pharmacol.* 2002; 135: 555-563.
29. Nii-Kono T, Iwasaki Y, Uchida M, Fujieda A, Hosokawa A, Motojima M, Yamato H, Kurokawa K, Fukagawa M. Indoxyl sulfate induces skeletal resistance to parathyroid hormone in cultured osteoblastic cells. *Kidney Int.* 2007; 71: 738-743.
30. Gu SS, Zhang Y, Wu SY, Diao TY, Gebru YA, Deng HW. Early molecular responses of bone to obstructive nephropathy induced by unilateral ureteral obstruction in mice. *Nephrology (Carlton).* 2012; 17: 767-773.
31. Li YC, Kong J, Wei M, Chen ZF, Liu SQ, Cao LP. 1,25-dihydroxyvitamin D(3) is a negative endocrine regulator of the renin-angiotensin system. *J Clin Invest.* 2002; 110: 229–238.
32. Mitani H, Ishizaka N, Aizawa T, Ohno M, Usui S, Suzuki T, Amaki T, Mori I, Nakamura Y, Sato M, Nangaku M, Hirata Y, Nagai R. *In vivo* klotho gene transfer ameliorates angiotensin II-induced renal damage. *Hypertension.* 2002; 39: 838-843.
33. Arneson TJ, Li S, Liu J, Kilpatrick RD, Newsome BB, St Peter WL. Trends in hip fracture rates in US hemodialysis patients, 1993-2010. *Am J Kidney Dis.* 2013; 62: 747-754.
34. Wakasugi M, Kazama JJ, Wada A, Hamano T, Masakane I, Narita I. Hip Fracture Trends in Japanese Dialysis Patients, 2008-2013. *Am J Kidney Dis.* 2018; 71: 173-181.

35. Hanna IR, Taniyama Y, Szöcs K, Rocic P, Griendling KK. NAD(P)H oxidase-derived reactive oxygen species as mediators of angiotensin II signaling. *Antioxid Redox Signal.* 2002; 4: 899-914.

36. van Oers RF, Wang H, Bacabac RG. Osteocyte shape and mechanical loading. *Curr Osteoporos Rep.* 2015; 13: 61-66.

37. Kimura Y, Matsugaki A, Sekita A, Nakano T. Alteration of osteoblast arrangement via direct attack by cancer cells: New insights into bone metastasis. Sci Rep. 2017; 7: 44824.

38. Saito M, Marumo K. Effects of Collagen Crosslinking on Bone Material Properties in Health and Disease. *Calcif Tissue Int.* 2015; 97: 242-261.

39. Chen NX, Srinivasan S, O'Neill K, Nickolas TL, Wallace JM, Allen MR, Metzger CE, Creecy A, Avin KG, Moe SM. Effect of advanced glycation end-products (AGE) lowering drug ALT-711 on biochemical, vascular, and bone parameters in a rat model of CKD-MBD. *J Bone Miner Res.* 2020; 35: 608-617.

40. NIH Consensus Development Panel on Osteoporosis Prevention, Diagnosis, and Therapy. Osteoporosis prevention, diagnosis, and therapy. *JAMA.* 2001; 285: 785-795. .

41. Kazama JJ, Iwasaki Y, Fukagawa M. Uremic osteoporosis. *Kidney Int Suppl (2011).* 2013; 3: 446-450.

42. Kazama JJ. Chronic kidney disease and fragility fracture. *Clin Exp Nephrol.* 2017; 21(Suppl 1): 46-52.

43. Moe SM. Renal Osteodystrophy or Kidney-Induced Osteoporosis? *Curr Osteoporos Rep.* 2017; 15: 194-197.

44. Gu SS, Zhang Y, Li XL, Wu SY, Diao TY, Hai R, Deng HW. Involvement of the Skeletal Renin-Angiotensin System in Age-Related Osteoporosis of Ageing Mice. *Biosci Biotechnol Biochem.* 2012; 76: 1367-1371.

Figure legends

Figure 1. Relationship between time to hospitalization due to fracture and clinical factors.

Association between CKD-MBD-related clinical parameters and the incidence of hospitalization due to (A) any fracture, and (B) that due to hip fracture. Multivariate-adjusted Cox proportional hazard models were used to estimate hazard ratios (HRs) and their 95% confidence intervals (CIs). In the multivariate analysis, the following covariates were adjusted for: age, sex, body mass index, causes of chronic kidney disease (CKD), smoking, history of parathyroidectomy, duration of dialysis, serum levels of albumin, calcium, phosphorus, intact parathyroid hormone (iPTH), and alkaline phosphatase, blood hemoglobin, prescriptions of type-I angiotensin II receptor blockade (AT-1RB), angiotensin converting enzyme inhibitor (ACEi), vitamin D receptor activators (VDRA), and phosphate binders.

Figure 2. Improvement in the kidney damage- induced increase of empty lacunae in cortical bone after Olmesartan treatment.

Bone histology showing the number of empty lacunae in cortical bone (N.Empty Lc/mm^2) in a rat model. C: control groups, N: nephrectomy groups, NO: nephrectomy with olmesartan groups, and NH: nephrectomy with hydralazine groups. A, H: natural light microscopy findings, B: fluorescence microscopy findings. White arrows show intact osteocytes, and yellow arrows show empty lacunae. Bars=10 mm. G: quantitative comparison of the number of empty lacunae among groups.

Figure 3. Effect of olmesartan on nephrectomy-induced bone chemical composition in a rat model.

(A) mineral-to-matrix ratio; (B) carbonate-to-phosphate ratio; (C) crystallinity; (D) crosslinks; (E) pentosidine-to-matrix ratio in C (control groups), N (nephrectomy groups), NO (nephrectomy with olmesartan groups) and NH (nephrectomy with hydralazine groups) are shown.

Figure 4. Expression of angiotensin II type I receptor 1 (AT-1R) in primary cultured osteocytes.

Cells were treated with different concentrations of angiotensin II for 24h.

AT-1R expression was assayed by real-time reverse transcription PCR. Fold induction of AT-1R gene expression was compared with beta-actin. Data are obtained from three independent experiments. P value: *vs* 0 mM AII.

Figure 5. Effect of angiotensin II on the viability of primary osteocytes

Primary cultured osteocytes were exposed to several concentrations of angiotensin II (AII) for 24h (A), 48h (B), and 96f (C). Cell viability decreased in a dose-dependent manner after a 96 h exposure to AII. P value: *vs* 0 mM AII.

Figure 6. Effect of angiotensin II on reactive oxygen spices (ROS) production in primary osteocytes

Angiotensin II induced ROS production in primary osteocytes in a dose-dependent manner

P value: *vs* 0 mM AII.

Figure 7. Improvement in angiotensin II-induced cell death and ROS production in osteocytes after Olmesartan treatment.

Primary cultured osoteocytes in the presence of 1000μM angiotensin II reacted with 10μM olmesartan (+O), 30μM hydralazine (+H), 2.5mM N-acetyl cysteine (+NAC), 0.5μM diphenyleneiodonium (+DPI), or without drugs (C). Cell viability (A), ROS production (B), DNA fragmentation (C), and NADPH oxidase expression including p22phox (D) and p67phox (E) were assessed, respectively. Each data was compared with that of angiotensin II non-treated cells and expressed as fold changes or increase. Data are presented as mean + standard deviation of three independent experiments. P value: *vs* C.

Figure 8. Hypothetical mechanism of bone fragility caused by decreased kidney function and the role of AT-1RB

Table 1 Characteristics of the analysis sample

Table 2 Demographic, bone histomorphometric and bone mechanical property in rat model

Table 1. Characteristics of the analysis sample

		Hospitalization due to any fracture		
	All	No	Yes	
Variable	N=3276	N=3098	N=178	p
Demographic and Clinical characteristics				
Age, years	63 (54-71)	62 (54-71)	69 (60-76)	<.001
Sex, female	38.5%	37.8%	50.6%	.001
Body mass index, kg/m^2	20.9 (19.0-23.3)	20.9 (19.1-23.3)	20.2 (18.3-23.1)	.031
Cause of ESKD				
Glomerulonephritis	44.9%	45.0%	43.3%	
Diabetic nephropathy	24.2%	23.8%	31.5%	
Nephrosclerosis	5.8%	5.9%	5.1%	
Others	25.2%	25.5%	20.3%	
Co-morbid conditions				
Diabetes mellitus	31.3%	31.0%	37.6%	.062
Cardiovascular disease	60.0%	59.7%	65.2%	.146
Dialysis				
Vintage, years	8.3 (3.8-14.3)	8.3 (3.8-14.3)	7.6 (2.9-13.7)	.689
Kt/V	1.41 (1.23-1.58)	1.41 (1.23-1.57)	1.45 (1.25-1.61)	.232
Laboratory data				
Albumin (g/dl)	3.8 (3.5-4.0)	3.8 (3.5-4.0)	3.7 (3.4-3.9)	.671
Calcium (mg/dl)	9.4 (8.9-10.1)	9.4 (8.9-10.1)	9.4 (8.8-10.0)	.856
Phosphate (mg/dl)	5.5 (4.6-6.3)	5.5 (4.6-6.3)	5.3 (4.5-6.2)	.275
intact PTH (pg/ml)	265 (195-392)	267 (196-394)	242 (192-338)	.926
Alkaline phosphatase (IU/l)	252 (197-330)	252 (197-329)	254 (196-353)	.188
medication				
AT-1RB	35.4%	36.0%	24.7%	.002
Calcium channel blocker	43.7%	43.8%	41.6%	.560
VDRA	48.7%	48.8%	46.6%	.567
Phosphate binder	85.3%	85.4%	84.8%	.851

ESKD; endstage kidney disease, PTH; parathyroid hormone, AT-1RB; angiotensin II type-I receptor blockade, VDRA; vitamin D receptor agonist

Table 2. Demographic, bone histomorphometric and bone mechanical property in rat model

Group		C (N=6)	N (N=8)	NO (N=9)	NH (N=6)
Body Weight	(g)	647.0±45.4	545.5±67.4 [a]	528.9±48.6 [a]	533.3±43.7 [a]
MBP	(mmHg)	110.8±13.5	148.9±13.9 [a]	114.9±28.9 [b]	116.8±10.9 [b]
Biochemistry					
Urea nitrogen	(mg/dl)	30.6±4.3	103.8±24.7 [a]	99.0±55.3 [a]	101.0±25.6 [a]
Creatinine	(mg/dl)	0.5±0.1	1.7±0.3 [a]	1.6±0.8 [a]	1.7±0.8 [a]
Calcium	(mg/dl)	10.7±1.6	11.1±1.1	11.6±0.9	11.5±0.7
Phosphate	(mg/dl)	7.8±1.1	7.8±1.4	7.9±1.9	7.2±2.0
intact PTH	(pg/dl)	109.5±129.3	1141.6±830.6	894.0±429.5 [a]	679.0±291.9
BMD	(mg/cm^3)	177.5±6.8	160.2±6.6 [a]	151.2±15.6 [a]	149.7±12.1 [a]
Bone histomorphometry					
ES/BS	(%)	5.9±2.1	10.7±3.4 [a]	9.8±5.3 [a]	10.8±7.2 [a]
N.Oc/B.Pm	(/mm)	1.5±0.6	2.0±0.7	2.5±0.8 [a]	2.3±0.5 [a]
Ob.S/BS	(%)	4.6±2.7	14.1±2.8 [a]	16.5±7.3 [a]	13.7±3.6 [a]
OS/BS	(%)	7.3±4.0	26.8±13.5 [a]	29.6±14.5 [a]	30.7±15.7 [a]
Elastic bone mechanical property					
Storage module	(Pa)	$7.7x10^9±2.5x10^8$	$2.5x10^9±7.9x10^8$ [a]	$3.5x10^9±4.6x10^8$ [a,b,c]	$1.5x10^9±8.3x10^8$ [a]
Tan delta		0.064±0.0012	0.061±0.017	0.060±0.010	0.056±0.021
Bone apatite orientation		6.9±0.3	5.4±0.6 [a]	6.8±0.2 [b,c]	6.6±0.3 [a]

C: control group, N: nephrectomy group, NO: nephrectomy with olmesaltan group, NH: nephrectomy with hydralazine group,

MBP: mean blood pressure, BMD: bone mineral density, BS: bone surface, ES: eroded surface, N.Oc: osteoclast number, Ob.S: osteoblastic surface, OS: osteoid surface, a; $p<0.05$ vs C, b; $p<0.05$ vs N, c; $p<0.05$ vs NH

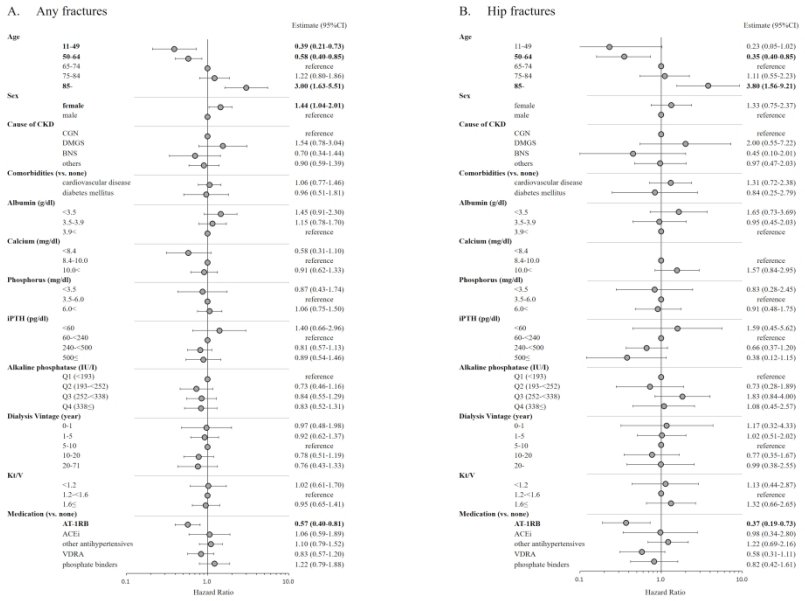

Figure 1. Relationship between time to hospitalization due to fracture and clinical factors. Association between CKD-MBD-related clinical parameters and the incidence of hospitalization due to (A) any fracture, and (B) that due to hip fracture. Multivariate-adjusted Cox proportional hazard models were used to estimate hazard ratios (HRs) and their 95% confidence intervals (CIs). In the multivariate analysis, the following covariates were adjusted for: age, sex, body mass index, causes of chronic kidney disease (CKD), smoking, history of parathyroidectomy, duration of dialysis, serum levels of albumin, calcium, phosphorus, intact parathyroid hormone (iPTH), and alkaline phosphatase, blood hemoglobin, prescriptions of type-I angiotensin II receptor blockade (AT-1RB), angiotensin converting enzyme inhibitor (ACEi), vitamin D receptor activators (VDRA), and phosphate binders.

651x425mm (300 x 300 DPI)

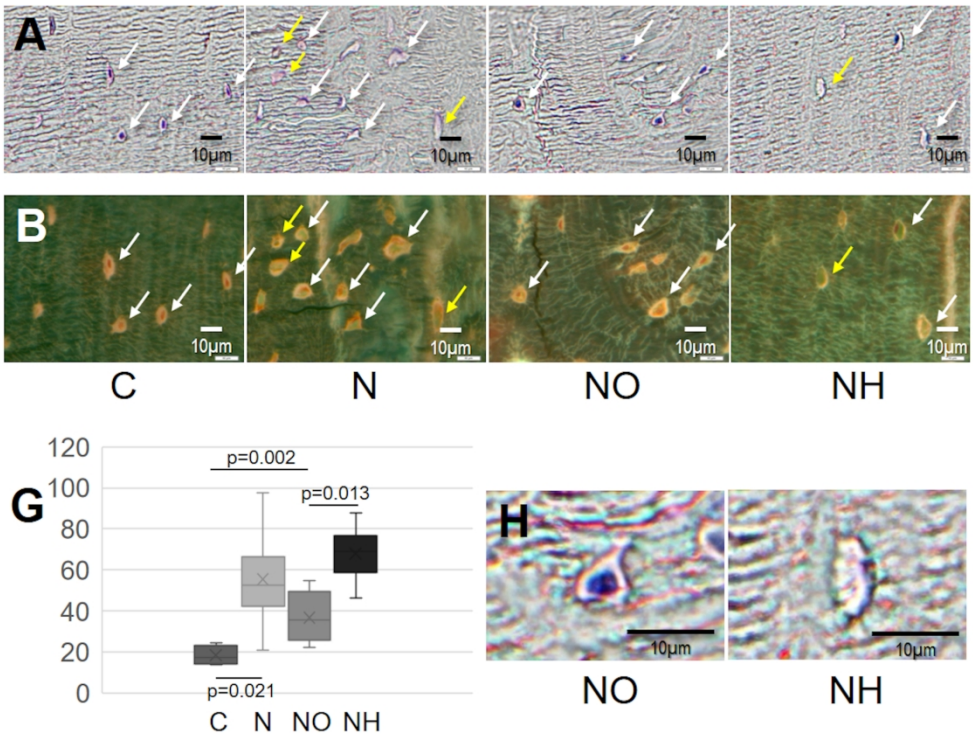

Figure 2. Improvement in the kidney damage- induced increase of empty lacunae in cortical bone after Olmesartan treatment.
Bone histology showing the number of empty lacunae in cortical bone (N.Empty Lc/mm2) in a rat model. C: control groups, N: nephrectomy groups, NO: nephrectomy with olmesartan groups, and NH: nephrectomy with hydralazine groups. A, H: natural light microscopy findings, B: fluorescence microscopy findings. White arrows show intact osteocytes, and yellow arrows show empty lacunae. Bars=10 mm. G: quantitative comparison of the number of empty lacunae among groups.

185x141mm (300 x 300 DPI)

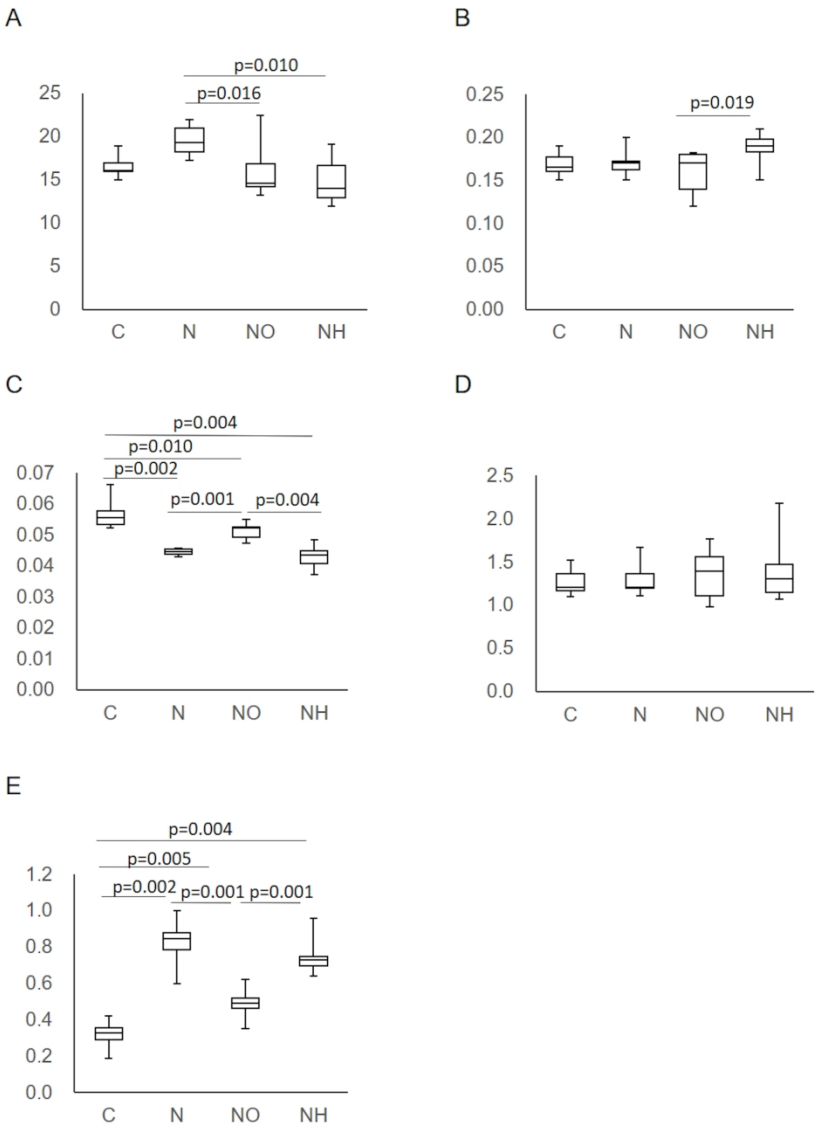

Figure 3. Effect of olmesartan on nephrectomy-induced bone chemical composition in a rat model. (A) mineral-to-matrix ratio; (B) carbonate-to-phosphate ratio; (C) crystallinity; (D) crosslinks; (E) pentosidine-to-matrix ratio in C (control groups), N (nephrectomy groups), NO (nephrectomy with olmesartan groups) and NH (nephrectomy with hydralazine groups) are shown.

181x239mm (300 x 300 DPI)

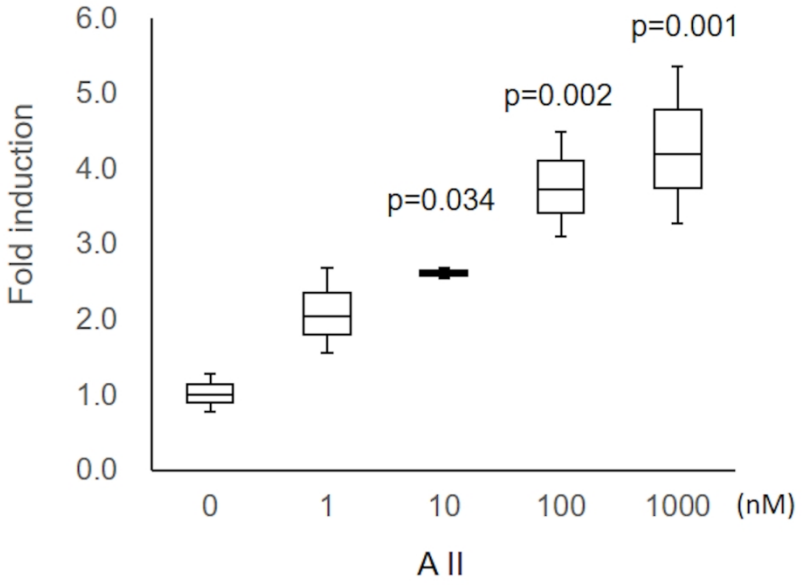

Figure 4. Expression of angiotensin II type I receptor 1 (AT-1R) in primary cultured osteocytes. Cells were treated with different concentrations of angiotensin II for 24h. AT-1R expression was assayed by real-time reverse transcription PCR. Fold induction of AT-1R gene expression was compared with beta-actin. Data are obtained from three independent experiments. P value: vs 0 mM AII.

129x108mm (300 x 300 DPI)

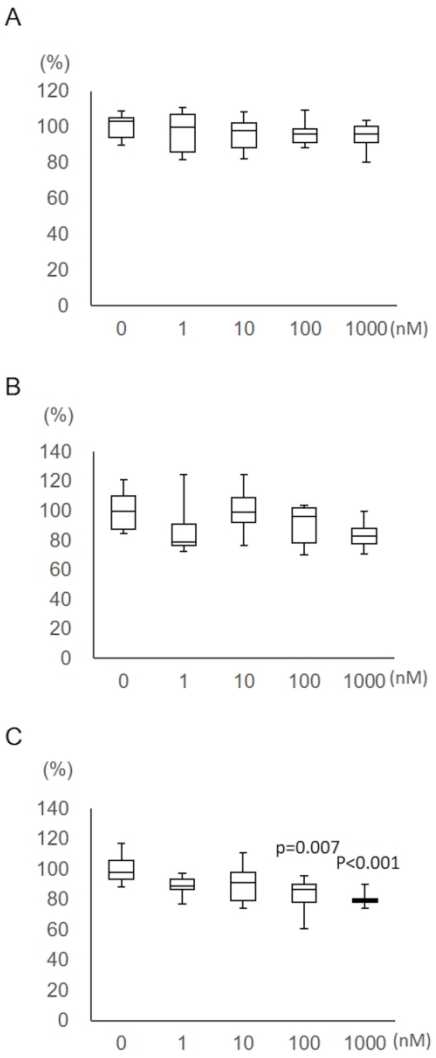

Figure 5. Effect of angiotensin II on the viability of primary osteocytes
Primary cultured osteocytes were exposed to several concentrations of angiotensin II (AII) for 24h (A), 48h (B), and 96f (C). Cell viability decreased in a dose-dependent manner after a 96 h exposure to AII. P value: vs 0 mM AII.

122x238mm (300 x 300 DPI)

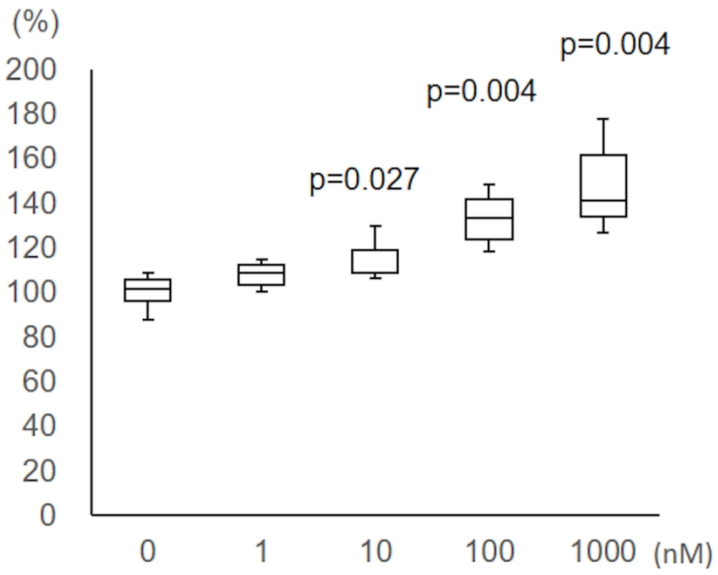

Figure 6. Effect of angiotensin II on reactive oxygen spices (ROS) production in primary osteocytes
Angiotensin II induced ROS production in primary osteocytes in a dose-dependent manner
P value: vs 0 mM AII.

126x117mm (300 x 300 DPI)

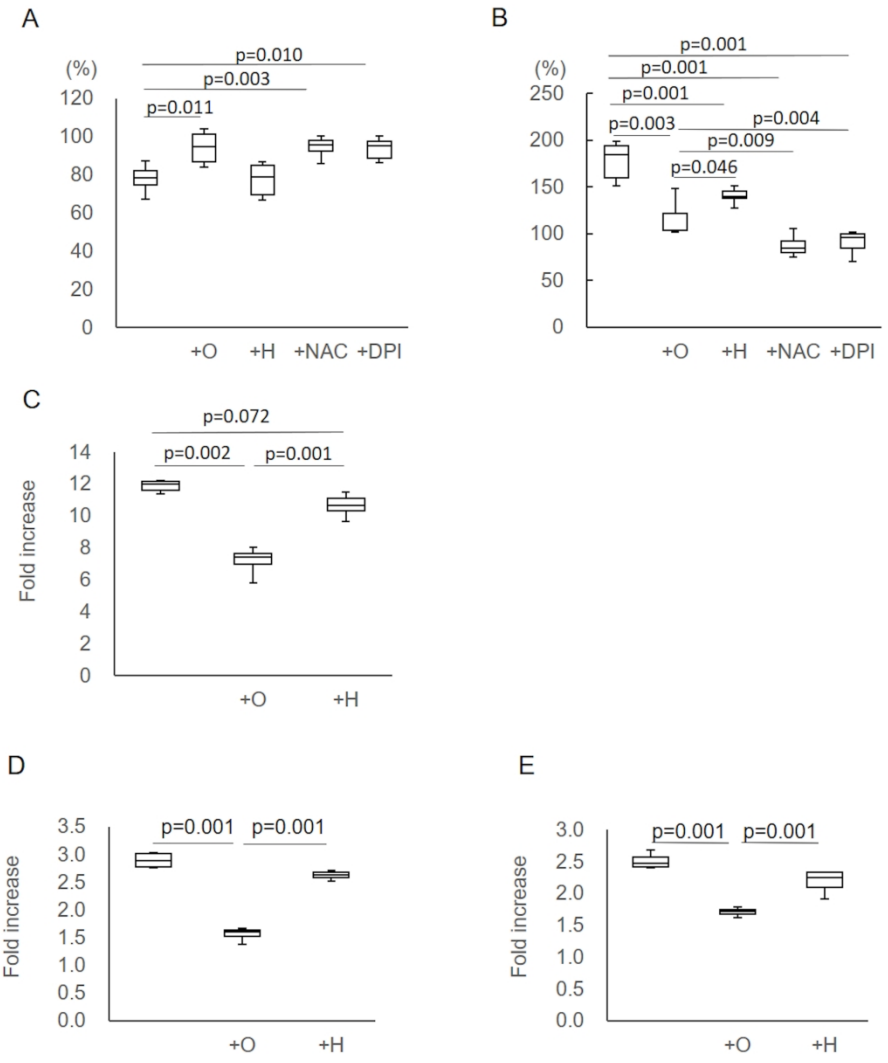

Figure 7. Improvement in angiotensin II-induced cell death and ROS production in osteocytes after Olmesartan treatment.

Primary cultured osoteocytes in the presence of 1000μM angiotensin II reacted with 10μM olmesartan (+O), 30μM hydralazine (+H), 2.5mM N-acetyl cysteine (+NAC), 0.5μM diphenyleneiodonium (+DPI), or without drugs (C). Cell viability (A), ROS production (B), DNA fragmentation (C), and NADPH oxidase expression including p22phox (D) and p67phox (E) were assessed, respectively.

Each data was compared with that of angiotensin II non-treated cells and expressed as fold changes or increase. Data are presented as mean + standard deviation of three independent experiments.

P value: vs C.

182x228mm (300 x 300 DPI)

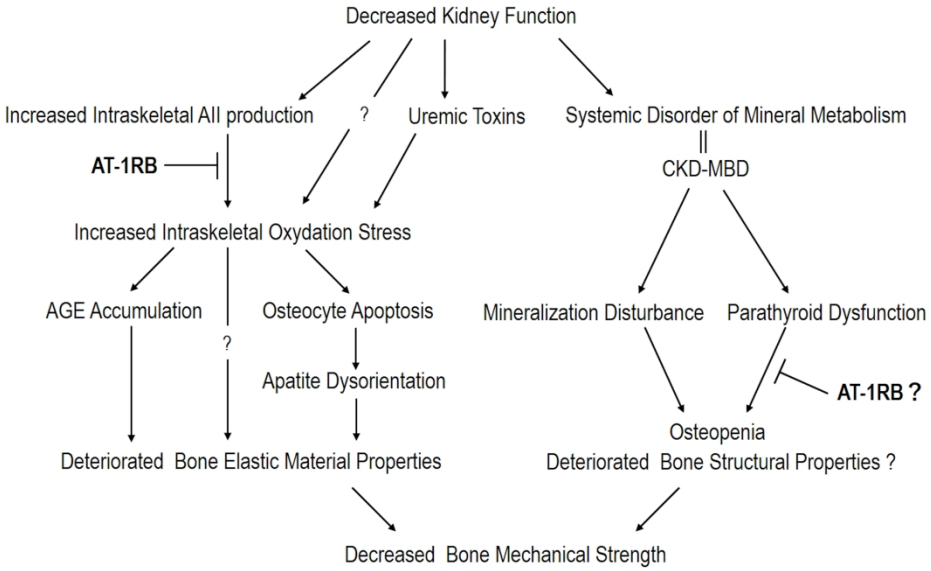

Figure 8. Hypothetical mechanism of bone fragility caused by decreased kidney function and the role of AT-1RB

277x192mm (300 x 300 DPI)